Chiral Instabilities and the Fate of Chirality Imbalance in Non-Abelian Plasmas

Sören Schlichting[1,*] and Sayantan Sharma[2,†]

[1]*Fakultät für Physik, Universität Bielefeld, D-33615 Bielefeld, Germany*
[2]*The Institute of Mathematical Sciences, a CI of Homi Bhabha National Institute, Chennai 600113, India*

We present a microscopic study of chiral plasma instabilities and axial charge transfer in non-Abelian plasmas with a strong gauge-matter coupling $g^2 N_f = 64$, by performing $3 + 1$D real-time classical-statistical lattice simulation with dynamical fermions. We explicitly demonstrate for the first time that—unlike in an Abelian plasma—the transfer of chirality from the matter sector to the gauge fields occurs predominantly due to topological sphaleron transitions. We elaborate on the similiarities and differences of the axial charge dynamics in cold Abelian U(1) and non-Abelian SU(2) plasmas, and comment on the implications of our findings for the study of anomalous transport phenomena, such as the chiral magnetic effect in QCD matter.

Introduction.—Novel transport phenomena in the presence of chiral fermions have received a considerable amount of attention with manifestations from high-energy physics to condensed matter systems [1–4]. Specifically, the emergence of the chiral magnetic effect (CME) [5–9] has been widely investigated in recent years, as a possible way to provide insights into the dynamics of topological structures in quantum chromodynamics (QCD) [10] or to realize transport phenomena in Dirac or Weyl semimetals [11–16].

Generically, such anomalous transport phenomena rely on the presence of a net chirality or axial charge imbalance $j_5^0 \neq 0$ in the fermion sector. However, due to quantum effects, the axial current $j_5^\mu = (j_5^0, \vec{j}_5)$ is not conserved, as expressed by the anomaly relation [17–19]

$$\partial_\mu j_5^\mu = -\frac{g^2 N_f}{2\pi^2} \mathrm{tr}[\mathbf{E} \cdot \mathbf{B}] \qquad (1)$$

valid for N_f degenerate flavors of massless Dirac fermions in the presence of dynamical gauge fields. Notably the expression $(g^2/4\pi^2)\mathrm{tr}[\mathbf{E} \cdot \mathbf{B}]$ on the right-hand side can be expressed as the divergence $\partial_\mu K^\mu$ of the Chern-Simons current K^μ describing the net helicity of the gauge fields, such that Eq. (1) effectively describes the conservation of the combined net chirality of fermions and helicity of gauge fields. Since by virtue of Eq. (1) the axial charge density j_5^0 in the fermion sector is manifestly not conserved, a crucial

aspect of anomalous transport is therefore to understand how exactly and on what timescale the net chirality is transferred between fermionic and the gauge degrees of freedom.

Specifically, in the context of Abelian gauge theories such as quantum electrodynamics (QED), it is well established [20–23] that fluctuations of the electric, and magnetic fields can deplete the net axial charge density in the system, thus requiring the application of external electromagnetic (EM) fields to sustain anomalous transport phenomena [24] such as the CME in condensed matter systems [25]. Conversely, in electromagnetic plasmas where no external fields are applied, any net chirality imbalance in the fermion sector is eventually transferred to the gauge field sector. Based on a series of studies based on weak-coupling techniques [21,22,26,27], effective macroscopic descriptions [20,28,29] as well as nonperturbative real-time lattice simulation [23,30,31], it has been established that the chirality transfer proceeds via an exponential growth (and decay) of right- (left-) handed helical magnetic field modes due to the so-called chiral plasma instability [32]. Eventually, the unstable growth saturates, leading to a self-similar turbulent cascade that results in the generation of large scale helical magnetic fields [20,23,33].

Despite the fact that different theoretical approaches are able to describe the dynamics of chirality transfer in Abelian gauge theories, the theoretical description of chirality transfer processes in non-Abelian gauge theories, such as QCD or the electroweak sector of the standard model, is significantly more involved. Because of the nontrivial structure of the gauge group, non-Abelian SU(N_c) gauge theories possess an infinite number of physically equivalent configurations whose vacua are topologically distinct [34,35], which differ from each other by an integer amount of the chiral charge $N_{\mathrm{CS}} = \int_{\mathbf{x}} K^0$.

Nonperturbative real-time processes can lead to so-called sphaleron transitions between the different topological sectors [36,37], which tend to erase any preexisting chiral charge imbalance in the fermion sector [38,39], such that ultimately one expects all chiral charge to be absorbed into the topology of the non-Abelian gauge fields. Despite the fact that such processes are not only important for understanding the real-time dynamics of anomalous transport phenomena, but also play a crucial role in different scenarios of baryo- or leptogenesis in the early Universe [40–42], a microscopic theoretical description is complicated by the interplay of several scales [43], and one typically resorts to effective macroscopic descriptions in the form of hydrodynamic equations [44–49] or classical effective theories [50–52].

In this Letter, we report on the first microscopic study of chirality transfer in non-Abelian plasmas. Specifically, we investigate the dynamics of chiral plasma instabilities and chirality transfer in an environment where the ambient temperature is much lower than the initial helicity chemical potential. Unlike at weak coupling and high temperatures where the primary unstable modes reside at magnetic scale, there is no natural separation of scales in this regime. Starting from a large helicity imbalance in the fermion sector, we employ a classical-statistical description [53–57] to simulate the subsequent nonequilibrium evolution of the system. Beginning with the early onset of exponentially growing primary instabilities, we follow the evolution of the system to the highly nonlinear regime where the unstable growth saturates and chirality transfer from the fermion to the gauge sector proceeds as anticipated via a sequence of correlated sphaleron transitions. We explicitly demonstrate that chirality transfer in non-Abelian plasmas is primarily driven by such topological transitions and comment on the consequences of our findings for the emergence of anomalous transport phenomena such as the CME in non-Abelian plasmas.

Simulation setup.—We perform real-time simulation of N_f degenerate flavors of Dirac fermions of mass m, coupled to classical-statistical non-Abelian SU(N_c) gauge fields [58–63]. We numerically solve the coupled set of Dirac equations

$$i\partial_t \hat{\Psi}_{\mathbf{x}}(t) = \gamma^0(-i\gamma^i D_i[A] + m)\hat{\Psi}_{\mathbf{x}}(t), \tag{2}$$

for the fermion fields $\hat{\Psi}_{\mathbf{x}}(t)$, where $D^i[A] \equiv \partial^i - igA^i_{\mathbf{x}}(t)$ is the covariant derivative in temporal-axial ($A_0 = 0$) gauge, and the Yang-Mills equations for the non-Abelian gauge fields $\mathbf{E}^a_{\mathbf{x}}(t)$ and $\mathbf{B}^a_{\mathbf{x}}(t)$,

$$\partial_t g\mathbf{E}^a_{\mathbf{x}}(t) - [\mathbf{D} \times g\mathbf{B}_{\mathbf{x}}(t)]^a = -g^2 N_f \mathbf{j}^a_{\mathbf{x}}(t). \tag{3}$$

Evolution equations (2) and (3) include the effects of color fields on the fermion sector as well as the nonlinear backreaction of fermion currents $\mathbf{j}^a_{\mathbf{x}}(t) = \langle \frac{1}{2}[\hat{\Psi}^\dagger_{\mathbf{x}}(t)t^a\gamma^0\boldsymbol{\gamma}, \hat{\Psi}_{\mathbf{x}}(t)]\rangle$,

on the dynamical evolution on the non-Abelian fields in Eq. (3). We note that the classical-statistical description in Eqs. (2) and (3) is accurate to leading order in the gauge coupling g^2, but to all orders in the coupling $g^2 N_f$ between matter and gauge fields [58,60]. In this work we focus on the simplest non-Abelian gauge group SU(2) and employ $g^2 N_f = 64$ to implement a strong backreaction of the matter fields to the gauge fields. This allows us not only to properly resolve all relevant scales of the problem, but also to investigate the mechanism of the chirality transfer beyond the weak-coupling limit [32,51].

We formulate the problem on a N_s^3 spatial lattice with lattice spacing a_s, using a compact Hamiltonian lattice formulation of SU(2) gauge theory [64], with $O(a_s^3)$ tree-level improved Wilson fermions [63] which is essential for realizing the chiral anomaly with a good precision on a finite size lattice. Clearly, the implementation of the fermion field operator $\hat{\Psi}_{\mathbf{x}}(t)$ is the most expensive part of our numerical algorithm as the solution to the operator Eq. (2) is constructed from linear combinations of a complete set of $8N_s^3$ wave functions [58,63].

We will analyze the nonequilibrium evolution of a chirally imbalanced charge neutral ensemble of fermions, by specifying the initial occupation numbers of left- (L) and right- (R) handed fermions at $t = 0$ according to a Fermi-Dirac distribution $n_F^{L/R}(t=0,\mathbf{p}) = [1/(e^{(E_\mathbf{p} \pm \mu_h)/T} + 1)]$ with a helicity chemical potential μ_h and energy $E_\mathbf{p} = \pm\sqrt{\mathbf{p}^2 + m^2}$ for particles and antiparticles, respectively. The initial conditions for the gauge fields are chosen as a classical-statistical ensemble representing vacuum fluctuations [23,65]. We focus on the dynamics in a cold and dense plasma with an initial $T/\mu_h = 1/8$ to make a comparison with our earlier studies of an Abelian plasma [23] and please refer to the Supplemental Material of [23] for additional details of the implementation. To estimate the residual effects of finite lattice spacing and lattice size, we have performed variations of $\mu_h a_s = 0.8$–1.0 and $N_s = 24$–40 and if not stated otherwise, we will present results for our largest and finest lattices with $N_s = 40$ and $\mu_h a_s = 0.8$. Simulations are performed close to the chiral limit $m \ll \mu_h$ by fixing $ma_s = 5 \times 10^{-4}$. We will express all results in the units of the only dimensionful scale, the helicity chemical μ_h. By appropriate choice of μ_h, this allows for a translation of the physical timescales in different physical settings. So, for instance, if in a cosmological setting $\mu_h = 100$ GeV and $T \ll \mu_h$ then the timescale $1/\mu_h \approx 0.002$ fm/c. Generally, changing from SU(2) to SU(N) can be expected to change the order one prefactors in the dynamics. Similarly, the dependence on the gauge coupling g is only logarithmic, as is typically the case for the dynamics of instabilities, so the only relevant parameter affecting the timescales is the gauge matter coupling $g^2 N_f$. While it would be interesting to investigate the dependence on $g^2 N_f$ further, the numerical cost of the
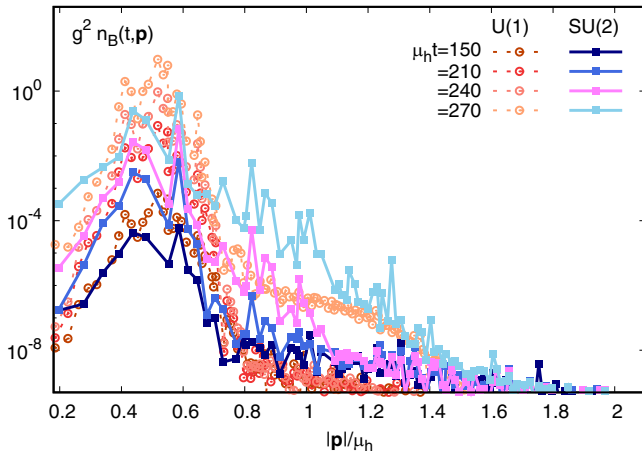
FIG. 1. Evolution of the (chromo-) magnetic field spectra $g^2 n_B(t, \mathbf{p})$ at early times $\mu_h . t < 300$ in an SU(2) plasma ($V = 32/\mu_h^3, \mu_h a_s = 0.8$) shown in shades of blue and a U(1) plasma ($V = 48/\mu_h^3, \mu_h a_s = 1$), shown in shades of orange. Chiral plasma instabilities lead to the exponential growth of right-handed magnetic field modes with momenta $|\mathbf{p}|/\mu_h \sim 0.5$ with comparable growth rates in SU(2) and U(1) plasmas.

FIG. 2. Evolution of the (chromo-) magnetic field spectra $g^2 n_B(t, |\mathbf{p}|)$ at late times $\mu_h . t > 300$ in an SU(2) plasma ($V = 32/\mu_h^3, \mu_h a_s = 0.8$) shown in shades of blue and a U(1) plasma ($V = 48/\mu_h^3, \mu_h a_s = 1$)), shown in shades of orange. Because of non-Abelian self-interactions the unstable growth saturates for the SU(2) plasma and the magnetic field occupation numbers do not exceed the nonperturbative threshold $n_B(t, |\mathbf{p}|) \sim 1/g^2$. Conversely, the Abelian U(1) plasma shows an inverse cascade of magnetic helicity, resulting in the generation of strong large scale coherent magnetic fields [23].

simulations prohibits a full exploration of the parameter space.

Chiral plasma instabilities.—We now proceed to analyze the mechanism of chirality transfer from fermions to gauge fields, and frequently contrast our findings for non-Abelian plasmas with earlier studies in Abelian gauge theories [23]. Starting from a large net chirality imbalance in the fermion sector, both Abelian and non-Abelian plasmas exhibit an instability [32] resulting in an exponential growth or suppression of right- or left-handed magnetic field modes at early times. We illustrate this behavior in Fig. 1, where we present the evolution of the spectrum of (chromo-) magnetic field modes

$$n_B(t, \mathbf{p}) = \frac{1}{\nu} \sum_{a=1}^{N_c} \frac{|\mathbf{B}^a(t, \mathbf{p})|^2}{|\mathbf{p}|}, \qquad (4)$$

where $\mathbf{B}^a(t, \mathbf{p}) = (1/\sqrt{V}) \int d^3\mathbf{x}\, \mathbf{B}^a(\mathbf{x}, t) e^{-i\mathbf{p}\cdot\mathbf{x}}$ is the Fourier transform of the (chromo-)magnetic field strength $\mathbf{B}^a(\mathbf{x}, t)$ extracted from elementary lattice plaquettes as in [23] and $\nu = (N_c^2 - 1)$ for SU(N_c) and $\nu = 1$ for the U(1) gauge group, respectively. [Since the magnetic field strength $\mathbf{B}^a(\mathbf{x}, t)$ transforms nontrivially under non-Abelian gauge transformations, we follow [55,66] and calculate the equal time correlation function in Eq. (4) in Coulomb gauge to minimize gauge artifacts.]

Starting from initial vacuum fluctuations, the chiral plasma instability results in a rapidly growing population of primarily unstable modes with $|\mathbf{p}|/\mu_h \lesssim 0.8$. Small momentum modes with $|\mathbf{p}|/\mu_h \sim 0.5$ feature the largest growth rates, resulting in a pronounced peak in the spectra. Since at early times $\mu_h t \lesssim 300$ the occupation numbers are

small, $g^2 n_B(t, \mathbf{p}) \ll 1$, such that the field strength remains perturbative, the qualitative behavior of the Abelian U(1) and non-Abelian SU(2) theories is essentially the same; the only notable exception is the earlier onset of secondary instabilities for the latter due to non-Abelian self-interactions [67] around $\mu_h t \sim 200$, which results in the population of higher momentum modes $|\mathbf{p}|/\mu_h \gtrsim 1$ for the SU(2) plasma.

Striking differences between the evolution in the Abelian and the non-Abelian plasma start to emerge for times $\mu_h t \gtrsim 300$ depicted in Fig. 2, where the occupation numbers become nonperturbatively large, $g^2 n_B \sim 1$, and the dynamics becomes highly nonlinear. Specifically, for the SU(2) gauge theory, the non-Abelian self-interactions of the gauge fields lead to saturation of the unstable growth once the occupation numbers n_B of unstable modes become on the order of the inverse self-coupling $\sim 1/g^2$ [67,68]. While at intermediate times $\mu_h t \sim 300$ interactions between unstable modes produce distinct peaks in the spectrum at integer multiples of the momentum of the primarily unstable mode $|\mathbf{p}|/\mu_h \sim 0.5$ successive interactions lead to rapid population of the ultraviolet tails of the spectrum. Subsequently, for $\mu_h t \gtrsim 360$, the spectrum of the (chromo-)magnetic SU(2) fields features a large infrared occupation $n_B \sim 1/g^2$ for $|\mathbf{p}|/\mu_h \lesssim 0.5$ followed by a rapid decrease towards the ultraviolet and approximately retains this shape over the course of the entire evolution depicted in Fig. 2.

Conversely, in the case of the Abelian U(1) gauge theory, the growth of unstable modes only saturates at a later time leaving a pronounced peak in the spectrum around

$|\mathbf{p}|/\mu_h \sim 0.5$ for $\mu_h t \sim 360$. Subsequently, the characteristic peak moves towards lower and lower momenta, where in sharp contrast to the SU(2) plasma, infrared occupation numbers at late times $\mu_h t \gtrsim 360$ do exceed the nonperturbative threshold $n_B \gtrsim 1/g^2$. Strikingly, this behavior can be associated with a self-similar inverse cascade of the magnetic helicity, where the evolution of the spectrum can (approximately) be described in terms of universal scaling functions and scaling exponents [23]. Over the course of this process, the net axial charge of the fermions is transferred to the gauge field sector, and subsequently transported to lower and lower momentum scales, eventually resulting in the generation of long range helical magnetic fields [20,23,33].

Chirality transfer and fate of axial charge imbalance in non-Abelian plasmas.—Since in contrast to the Abelian U(1) plasma no long-range coherent fields are generated in the case of a non-Abelian SU(2) plasma (see also [55,68]) it becomes a crucial question to what extent and by which mechanism axial charge is transferred from fermions to gauge fields over the course of the instability dynamics. In order to investigate the chirality transfer mechanism in non-Abelian plasmas, it proves insightful to study the evolution of the Chern-Simons number

$$\Delta N_{\mathrm{CS}}(t) = \frac{g^2}{4\pi^2} \int_0^t dt' \int_{\mathbf{x}} \mathrm{Tr}[\mathbf{E}_{\mathbf{x}}(t') \cdot \mathbf{B}_{\mathbf{x}}(t')], \quad (5)$$

which represents the gauge field contribution to the anomaly budget in Eq. (1), such that when integrated over space the balance equation (1) for the axial charge takes the form (Note that strictly speaking this balance equation is only valid for N_f flavors of massless fermions. However, since in practice the fermion mass $m/\mu_h \ll 1$ is sufficiently small, finite mass effects are negligible over the timescales of our simulations and we have verified this explicitly by tracking the corresponding contribution to the anomaly budget.)

$$\frac{\Delta J_5^0(t)}{N_f} = -2\Delta N_{\mathrm{CS}}(t). \quad (6)$$

Our results for the chirality transfer in the non-Abelian SU(2) plasma are depicted in the top panel of Fig. 3, where we present the time evolution of the axial charge densities of fermions $[J_5^0/(VN_f)]$ and net helicity of gauge fields $[2\Delta N_{\mathrm{CS}}(t)/V]$. Different curves show the results for two different lattice discretizations ($N_s = 40$, $\mu_h a_s = 0.8$ and $N = 32$, $\mu_h a_s = 1$), indicating excellent convergence for ΔN_{CS}, whereas a sufficiently fine discretization is necessary to properly resolve the evolution of the axial charge of fermions J_5^0 and satisfy the anomaly relation in the lattice discretized theory (also see [63,69]). (We find that for $\mu_h a_s = 0.8$ residual violations of the anomaly relation are always below the $\sim$5% level even at late times $\mu_h t \gtrsim 500$.)
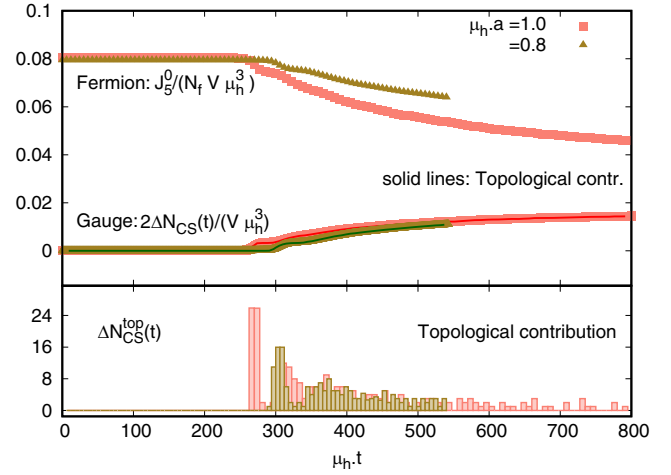
FIG. 3. (top) Evolution of the axial charge density of fermions $J_5^0/(N_f \mu_h^3 V)$ and gauge fields $2\Delta N_{\mathrm{CS}}/(\mu_h^3 V)$ in the SU(2) plasma. Different symbols show the results for two different lattice spacings $\mu_h a_s = 0.8$ (green) and $\mu_h a_s = 1$ (red), respectively. Changes in the Chern-Simons number ΔN_{CS} are predominantly due to nonequilibrium sphaleron transitions, as shown by the solid line, which contains the topological contribution obtained by cooling the non-Abelian gauge field configurations. (bottom) Change in the Chern-Simons number $\Delta N_{\mathrm{CS}}^{\mathrm{top}}(t)$ over a short time interval $\Delta t/a_s = 7.5$ due to topological transitions.

Starting around $\mu_h t \approx 300$ where the chiral plasma instability saturates, one observes an initially rapid transfer of chirality from fermions to gauge fields which subsequently slows down and continues over the course of the entire evolution in Fig. 3. While at first sight, the evolution of $J_5^0/(VN_f)$ and $2\Delta N_{\mathrm{CS}}(t)/V$, normalized in units of μ_h^3 in the non-Abelian plasma appears to be similar to the corresponding results in the Abelian U(1) case presented in [23], there is a crucial difference with regards to the nature of the configurations of the gauge fields that carry the net axial charge. Specifically it turns out that—in sharp contrast to Abelian gauge theories—the changes in Chern-Simons number can be attributed to the change in topology of the non-Abelian gauge field configurations emerging from a correlated sequence of sphaleron transitions. In order to isolate the topological contribution to ΔN_{CS}, we follow standard procedure and perform a gauge covariant cooling of the SU(2) gauge field configurations [70], which removes all excitations carrying a finite amount of energy while leaving the topology of the configuration untouched (see Appendix for details).

The bottom panel of Fig. 3 shows the change in Chern-Simons number $\Delta N_{\mathrm{CS}}^{\mathrm{top}}(t) = \Delta N_{\mathrm{CS}}^{\mathrm{cooled}}(t + \Delta t/2) - \Delta N_{\mathrm{CS}}^{\mathrm{cooled}}(t - \Delta t/2)$ due to topological transitions over a small time interval $\Delta t/a_s = 7.5$, and can essentially be understood as the (discrete) time derivative of the solid curves in the top panel (times $V\Delta t$). Because of its topological nature, this quantity is integer valued and represents the number of sphaleron transitions over the

time interval Δt. In contrast to thermal ensembles where individual sphaleron transitions are observed to be uncorrelated and the Chern-Simons number $\Delta N_{CS}(t)$ exhibits an integer random walk behavior (see, e.g., [70]), individual sphaleron transitions are highly correlated as all of them tend to erase the net axial charge in the fermion sector.

By inspecting the solid lines in the top panel, which represent the time integrated contribution to the Chern-Simons number from topological transitions $\sum_{t'<t} \Delta N_{CS}^{top}(t')$, we find that topological sphaleron transitions essentially account for the entire change in the Chern-Simons number. We therefore conclude from this analysis that on sufficiently large timescales, the initial axial charge imbalance is completely erased and absorbed by the topology of the non-Abelian gauge fields.

Conclusions and outlook.—In this Letter we report on the microscopic mechanism of the transfer of net chirality from the matter sector to the gauge field sector in a chirally imbalanced non-Abelian plasma. Based on classical-statistical lattice simulations close to the continuum limit, we can establish that the chirality transfer in non-Abelian plasmas occurs predominantly via topological transitions. Specifically, for the cold plasmas investigated in this study, the process is initiated by the onset of chiral plasma instabilities in the gauge field sector, which ultimately triggers very frequent sphaleron transitions, leading to a rapid transfer of chirality from the fermions to the gauge sector. Since the axial charge is absorbed by the topology of the gauge field, the gauge field occupancies do not exceed the scale $1/g^2$, and no coherent long-range magnetic fields are generated throughout the process. Strikingly, this is in sharp contrast to Abelian gauge theories, where as reported previously [23] a chirality imbalance in the fermion sector ultimately leads to the generation of large scale helical magnetic fields via an inverse turbulent cascade of the magnetic helicity. Conversely, in non-Abelian gauge theories the initial chirality imbalance is completely erased, and as the topologically distinct gauge field configurations are physically indistinguishable there is no physical effect on the evolution of the plasma on large timescales.

Our study provides the first explicit microscopic demonstration of the washout of an initial chiral charge imbalance due to topological transitions in a cold SU(2) plasma and has important implications for the study of anomalous transport phenomena which are driven by a net chirality imbalance in the fermion sector. Since the net chirality imbalance is ultimately erased, effects like the CME should be understood as transient nonequilibrium phenomena that persist only over a limited timescale.

Since unlike in the present study the QGP created in heavy-ion collisions is initially in a hot state with $T \gg \mu_h$, thus frequent changes of the topology of the gauge fields occur, even in the absence of an axial charge imbalance due to thermal sphaleron transitions [38]. In the presence of an axial charge imbalance in the fermion sector, sphaleron

transitions exhibit a bias, which just like in the present study, tends to erase the axial charge imbalance in the fermion sector, such that an initial charge imbalance decays on a timescale $\tau_{sph} = \chi_A T / \Gamma_{sph}$, where χ_A is the axial charge susceptibility and Γ_{sph} is the sphaleron transition rate [38]. Based on recent lattice estimates of $\Gamma_{sph} \sim 0.1 T^4$ [71,72] and the axial charge susceptibility of the pure gauge theory $\chi_A = N_c T^2 / 3$, this timescale is of the order of $\sim 10/T$ and we therefore anticipate that in heavy-ion collisions local pockets of nonzero net chirality created during the early nonequilibrium stages will slowly disappear, while at the same time more local regions of net chirality imbalance will be created due to finite temperature sphaleron transitions.

Evidently, a more detailed microscopic study of these competing phenomena in a QCD plasma will require the extension of our study to hot plasma, which requires us to disentangle the dynamics of the infrared modes $|\mathbf{p}| \lesssim g^2 T$ that are primarily responsible for chirality transfer from that of the (noisy) ultraviolet modes which reside at the scale $\sim T$ [50,51]. Since the ultimate fate of a chiral charge imbalance is quite different in Abelian and non-Abelian gauge theories, it would also be interesting to study these competing effects in theories like the standard model of particle physics, where matter fields are simultaneously coupled to both Abelian and non-Abelian gauge fields.

Appendix: Topological contribution to Cherns-Simons number.—We explain the extraction of the topological contribution to the change in the Chern-Simons number $\Delta N_{CS}^{top}(t)$. We follow [34] and employ gradient flow cooling of the three-dimensional gauge link configurations $U_{\mathbf{x},i}(t - \Delta t/2, \tau_c = 0)$ and $U_{\mathbf{x},i}(t + \Delta t/2, \tau_c = 0)$ up to a cooling time $\tau_c = 512 a_s^2$ by performing 4096 cooling steps with step size $\delta\tau_c / a_s^2 = 1/8$. Since each cooling step reduces the average field strength, this effectively

results in three-dimensional pure gauge configurations at the end of the cooling. Next, in order to compare the topology of the cooled configurations at times $t - \Delta/2$ and $t + \Delta t/2$ with $\Delta t/a_s = 7.5$, we connect the two independently cooled gauge configurations $U_{\mathbf{x},i}(t - \Delta t/2, \tau_c = 0)$ and $U_{\mathbf{x},i}(t + \Delta t/2, \tau_c = 0)$ via a geodesic interpolation on the SU(2) group manifold; i.e., we express

$$U_{\mathbf{x},i}\left(t + \frac{\Delta t}{2}, \tau_c\right) = e^{iga_s^2 \mathcal{E}_{\mathbf{x}}^a t_a \Delta t} U_{\mathbf{x},i}\left(t - \frac{\Delta t}{2}, \tau_c\right) \quad \text{(A1)}$$

and construct interpolating links

$$U_{\mathbf{x},i}(t + \theta \Delta t, \tau_c) = e^{iga_s^2 \mathcal{E}_{\mathbf{x}}^a t_a (\theta + \frac{1}{2}) \Delta t} U_{\mathbf{x},i}\left(t - \frac{\Delta t}{2}, \tau_c\right) \quad \text{(A2)}$$

for $-1/2 < \theta < 1/2$ to calculate the difference in the Chern-Simons number as

$$\begin{aligned}
\Delta N_{\text{CS}}^{\text{top}}(t) &= N_{\text{CS}}^{\text{cooled}}\left(t - \frac{\Delta t}{2}\right) - N_{\text{CS}}^{\text{cooled}}\left(t + \frac{\Delta t}{2}\right) \\
&= \frac{1}{8\pi^2} \frac{\Delta t}{a_s} \int_{-1/2}^{1/2} d\theta \sum_{\mathbf{x}} ga_s^2 \mathcal{E}_{\mathbf{x}}^a ga_S^2 \mathcal{B}_{\mathbf{x}}^a(t + \theta \Delta t)|_{\tau_c},
\end{aligned}$$
$$\text{(A3)}$$

where $\mathcal{E}_{\mathbf{x}}^a$ denote the fields in Eq. (A1), $\mathcal{B}_{\mathbf{x}}^a(t + \theta \Delta t)$ is the magnetic field strength associated with the interpolating gauge links in Eq. (A2). We employ an $\mathcal{O}(a_s^2)$ improved discretization of $\mathcal{E}$ and $\mathcal{B}$ [34,73], and calculate the integral over θ using Simpsons rule with $N_\theta = 16$ integration points.

Since Eq. (A3) provides the topological contribution to the change in Chern-Simons number ΔN_{CS} over the time interval $[t - \Delta t/2, t + \Delta t/2]$ shown in the bottom panel of Fig. 3, the topological contribution to the change in Chern-Simons number over the time interval $[0, t]$, shown in the top panel of Fig. 3, can then be computed as the sum over the configurations from each interval, i.e.,

$$\Delta N_{\text{CS}}(t)|_{\text{contribution}}^{\text{topological}} = \sum_{t' < t} \Delta N_{\text{CS}}^{\text{top}}(t'). \quad \text{(A4)}$$

[*]sschlichting@physik.uni-bielefeld.de
[†]sayantans@imsc.res.in

[1] A. Vilenkin, Phys. Rev. D **22**, 3080 (1980).
[2] D. E. Kharzeev, Prog. Part. Nucl. Phys. **75**, 133 (2014).
[3] V. A. Miransky and I. A. Shovkovy, Phys. Rep. **576**, 1 (2015).
[4] D. E. Kharzeev, arXiv:2204.10903.
[5] D. E. Kharzeev, L. D. McLerran, and H. J. Warringa, Nucl. Phys. **A803**, 227 (2008).
[6] K. Fukushima, D. E. Kharzeev, and H. J. Warringa, Phys. Rev. D **78**, 074033 (2008).
[7] D. E. Kharzeev, K. Landsteiner, A. Schmitt, and H.-U. Yee, Lect. Notes Phys. **871**, 1 (2013).
[8] D. E. Kharzeev, J. Liao, S. A. Voloshin, and G. Wang, Prog. Part. Nucl. Phys. **88**, 1 (2016).
[9] V. Koch, S. Schlichting, V. Skokov, P. Sorensen, J. Thomas, S. Voloshin, G. Wang, and H.-U. Yee, Chin. Phys. C **41**, 072001 (2017).
[10] D. E. Kharzeev and J. Liao, Nat. Rev. Phys. **3**, 55 (2021).
[11] D. T. Son and B. Z. Spivak, Phys. Rev. B **88**, 104412 (2013).
[12] E. V. Gorbar, V. A. Miransky, and I. A. Shovkovy, Phys. Rev. B **89**, 085126 (2014).
[13] Q. Li, D. E. Kharzeev, C. Zhang, Y. Huang, I. Pletikosic, A. V. Fedorov, R. D. Zhong, J. A. Schneeloch, G. D. Gu, and T. Valla, Nat. Phys. **12**, 550 (2016).
[14] A. Cortijo, D. Kharzeev, K. Landsteiner, and M. A. H. Vozmediano, Phys. Rev. B **94**, 241405(R) (2016).
[15] S. Kaushik, D. E. Kharzeev, and E. J. Philip, Phys. Rev. B **99**, 075150 (2019).
[16] P. O. Sukhachov, E. V. Gorbar, and I. A. Shovkovy, Phys. Rev. B **104**, L121113 (2021).
[17] S. L. Adler, Phys. Rev. **177**, 2426 (1969).
[18] J. S. Bell and R. Jackiw, Nuovo Cimento A **60**, 47 (1969).
[19] K. Fujikawa, Phys. Rev. D **21**, 2848 (1980); **22**, 1499(E) (1980).
[20] Y. Hirono, D. E. Kharzeev, and Y. Yin, Phys. Rev. D **92**, 125031 (2015).
[21] E. V. Gorbar, I. A. Shovkovy, S. Vilchinskii, I. Rudenok, A. Boyarsky, and O. Ruchayskiy, Phys. Rev. D **93**, 105028 (2016).
[22] K. Tuchin, Nucl. Phys. **A969**, 1 (2018).
[23] M. Mace, N. Mueller, S. Schlichting, and S. Sharma, Phys. Rev. Lett. **124**, 191604 (2020).
[24] M. Joyce and M. E. Shaposhnikov, Phys. Rev. Lett. **79**, 1193 (1997).
[25] E. V. Gorbar, V. A. Miransky, I. A. Shovkovy, and P. O. Sukhachov, Low Temp. Phys. **44**, 487 (2018).
[26] D. T. Son and N. Yamamoto, Phys. Rev. Lett. **109**, 181602 (2012).
[27] C. Manuel and J. M. Torres-Rincon, Phys. Rev. D **92**, 074018 (2015).
[28] K. Hattori, Y. Hirono, H.-U. Yee, and Y. Yin, Phys. Rev. D **100**, 065023 (2019).
[29] E. V. Gorbar, V. A. Miransky, I. A. Shovkovy, and P. O. Sukhachov, Phys. Rev. B **97**, 121105(R) (2018).
[30] P. V. Buividovich and M. V. Ulybyshev, Phys. Rev. D **94**, 025009 (2016).
[31] D. G. Figueroa, A. Florio, and M. Shaposhnikov, J. High Energy Phys. 10 (2019) 142.
[32] Y. Akamatsu and N. Yamamoto, Phys. Rev. Lett. **111**, 052002 (2013).
[33] I. Rogachevskii, O. Ruchayskiy, A. Boyarsky, J. Fröhlich, N. Kleeorin, A. Brandenburg, and J. Schober, Astrophys. J. **846**, 153 (2017).
[34] M. Mace, S. Schlichting, and R. Venugopalan, Phys. Rev. D **93**, 074036 (2016).
[35] F. Lenz, Lect. Notes Phys. **659**, 7 (2005).
[36] F. R. Klinkhamer and N. S. Manton, Phys. Rev. D **30**, 2212 (1984).

[37] R. F. Dashen, B. Hasslacher, and A. Neveu, Phys. Rev. D **10**, 4138 (1974).

[38] L. D. McLerran, E. Mottola, and M. E. Shaposhnikov, Phys. Rev. D **43**, 2027 (1991).

[39] J. M. Cline, K. Kainulainen, and K. A. Olive, Phys. Rev. Lett. **71**, 2372 (1993).

[40] V. A. Kuzmin, V. A. Rubakov, and M. E. Shaposhnikov, Phys. Lett. B **155**, 36 (1985).

[41] V. A. Rubakov and M. E. Shaposhnikov, Usp. Fiz. Nauk **166**, 493 (1996).

[42] D. Bodeker and W. Buchmuller, Rev. Mod. Phys. **93**, 035004 (2021).

[43] D. Bodeker, Phys. Lett. B **426**, 351 (1998).

[44] J. Erdmenger, M. Haack, M. Kaminski, and A. Yarom, J. High Energy Phys. 01 (2009) 055.

[45] D. T. Son and P. Surowka, Phys. Rev. Lett. **103**, 191601 (2009).

[46] R. Loganayagam, arXiv:1106.0277.

[47] D. E. Kharzeev and H.-U. Yee, Phys. Rev. D **84**, 045025 (2011).

[48] N. Banerjee, J. Bhattacharya, S. Bhattacharyya, S. Jain, S. Minwalla, and T. Sharma, J. High Energy Phys. 09 (2012) 046.

[49] M. Hongo, Y. Hirono, and T. Hirano, Phys. Lett. B **775**, 266 (2017).

[50] Y. Akamatsu and N. Yamamoto, Phys. Rev. D **90**, 125031 (2014).

[51] Y. Akamatsu, A. Rothkopf, and N. Yamamoto, J. High Energy Phys. 03 (2016) 210.

[52] N. Mueller and R. Venugopalan, Phys. Rev. D **96**, 016023 (2017).

[53] A. Polkovnikov, Ann. Phys. (Amsterdam) **325**, 1790 (2010).

[54] J. Berges, S. Schlichting, and D. Sexty, Phys. Rev. D **86**, 074006 (2012).

[55] A. Kurkela and G. D. Moore, Phys. Rev. D **86**, 056008 (2012).

[56] S. Jeon, Ann. Phys. (Amsterdam) **340**, 119 (2014).

[57] J. Berges, arXiv:1503.02907.

[58] G. Aarts and J. Smit, Nucl. Phys. **B555**, 355 (1999).

[59] J. Berges, D. Gelfand, and J. Pruschke, Phys. Rev. Lett. **107**, 061301 (2011).

[60] V. Kasper, F. Hebenstreit, and J. Berges, Phys. Rev. D **90**, 025016 (2014).

[61] N. Mueller, F. Hebenstreit, and J. Berges, Phys. Rev. Lett. **117**, 061601 (2016).

[62] N. Müller, S. Schlichting, and S. Sharma, Phys. Rev. Lett. **117**, 142301 (2016).

[63] M. Mace, N. Mueller, S. Schlichting, and S. Sharma, Phys. Rev. D **95**, 036023 (2017).

[64] J. B. Kogut and L. Susskind, Phys. Rev. D **11**, 395 (1975).

[65] G. Aarts and J. Berges, Phys. Rev. Lett. **88**, 041603 (2002).

[66] J. Berges, K. Boguslavski, S. Schlichting, and R. Venugopalan, Phys. Rev. D **89**, 114007 (2014).

[67] J. Berges, S. Scheffler, and D. Sexty, Phys. Rev. D **77**, 034504 (2008).

[68] A. Kurkela and G. D. Moore, J. High Energy Phys. 12 (2011) 044.

[69] L. H. Karsten and J. Smit, Nucl. Phys. **B183**, 103 (1981).

[70] G. D. Moore, Phys. Rev. D **59**, 014503 (1998).

[71] M. Barroso Mancha and G. D. Moore, J. High Energy Phys. 01 (2023) 155.

[72] L. Altenkort, A. M. Eller, O. Kaczmarek, L. Mazur, G. D. Moore, and H.-T. Shu, Phys. Rev. D **103**, 114513 (2021).

[73] G. D. Moore, Nucl. Phys. **B480**, 689 (1996).